J Solid State Electrochem (2011) 15:725–730
DOI 10.1007/s10008-010-1145-2

ORIGINAL PAPER

Preparation and performance comparison of $LiMn_2O_{3.95}Br_{0.05}$ and $LiMn_2O_{3.95}Br_{0.05}/SiO_2$ cathode materials for lithium-ion battery

Zhifang Dong · Yudai Huang · Dianzeng Jia · Zaiping Guo

Received: 8 March 2010 / Revised: 2 July 2010 / Accepted: 8 July 2010 / Published online: 22 July 2010

Abstract $LiMn_2O_{3.95}Br_{0.05}$ and $LiMn_2O_{3.95}Br_{0.05}/SiO_2$ cathode composites for lithium-ion battery are prepared by solid-state reaction methods. The crystalline structures of the as-synthesized samples are investigated by X-ray diffraction and transmission electron microscope; at the same time, the electrochemical performances are tested by cyclic voltammetry and galvanostatic cycling. The results reveal that the sample of $LiMn_2O_{3.95}Br_{0.05}/SiO_2$ has more excellent electrochemical performance than the sample of $LiMn_2O_{3.95}Br_{0.05}$. It delivers an initial discharge capacity of 145.3 $mAhg^{-1}$ at ambient temperature, and 138.9 $mAhg^{-1}$ at the higher temperature of 55 °C with good capacity retention with the voltage range of 3.0–4.35 V (vs. Li) at a current density of 0.5 C; while the sample of $LiMn_2O_{3.95}Br_{0.05}$ only deliver initial discharge capacity 136.5 $mAhg^{-1}$ at ambient temperature, and 119.2 $mAhg^{-1}$ at 55 °C in the same conditions; in addition, the rate performance of $LiMn_2O_{3.95}Br_{0.05}/SiO_2$ is excellent too, so the SiO_2 layer has improved the electrochemical behaviors of $LiMn_2O_{3.95}Br_{0.05}$ availably.

Keywords Lithium manganese oxide · SiO_2 layer · Cathode material · Lithium-ion battery

Z. Dong · Y. Huang · D. Jia (✉)
Institute of Applied Chemistry, Xinjiang University,
Urumqi 830046, People's Republic of China
e-mail: jdz0991@gmail.com

Z. Guo
School of Mechanical, Materials and Mechatronic Engineering,
University of Wollongong,
Wollongong, NSW 2522, Australia

Z. Guo
Institute for Superconducting and Electronic Materials,
University of Wollongong,
Wollongong, NSW 2522, Australia

Introduction

The present commercial lithium-ion battery involves graphite anode, a lithium cobalt oxide cathode, and a liquid organic-solution electrolyte. The $LiCoO_2$ has a theoretical capacity of 140 $mAhg^{-1}$, but the high cost, toxicity, and limited abundance of cobalt have been recognized to be disadvantage [1, 2]. The most promising alternative material is $LiMn_2O_4$ [3–7], due to its low cost, environmental friendliness, and the abundance of its raw materials in nature. However, $LiMn_2O_4$ still has difficulty in practical application, owing to its severe capacity decline. Many researchers have devoted much effort to overcome this problem. Several attempts have been made by doping the lithium manganese spinels with various metals, such as Al, Mg, Co, Ni, Cr, etc. [1, 8–10]. Although such substitutions often result in enhancing the stability of spinel, the initial discharge capacities of the doped-typed spinels decrease significantly and are lower than that of the parent compound. Lin et al. [6] have reported that surface coating with transition metal oxides have been shown as an effective way to improve the electrochemical performance for some cathode materials of lithium-ion battery.

In our previous work [11], the $LiMn_2O_4$ with Br doping have been investigated, the O^{2-} in the spinel phase are replaced by Br^-, and the substitution of monovalent Br^- for divalent O^{2-} results in the increasing of Mn^{3+} content in spinel, which contributes to charge–discharge capacity during intercalation–deintercalation of Li^+ in $LiMn_2O_4$, and Br^- doping brings in larger lattice constants of samples, thus, Li^+ can move more freely in the sample, and this might help increase the capacity. Zheng ZS et al. [2] have reported the surface modification of $Li_{1.03}Mn_{1.97}O_4$ with SiO_2, the SiO_2 coating layers hindered the dissolution of manganese into electrolyte solution, and improved the

electrochemical performance, and Song et al. [12] reported that the SiO_2 modification could enhance the behavior at elevated temperature. So, to further upgrade its electrochemical properties, herein, $LiMn_2O_{3.95}Br_{0.05}/SiO_2$ composites, with SiO_2 as surface coating material, were synthesized successfully by solid-state reaction methods. The crystalline structure and the electrochemical performance of the $LiMn_2O_{3.95}Br_{0.05}$ and $LiMn_2O_{3.95}Br_{0.05}/SiO_2$ samples were investigated. The results show that $LiMn_2O_{3.95}Br_{0.05}/SiO_2$ composites have improved the electrochemical performance with an initial discharge capacity of 145 $mAhg^{-1}$ at ambient temperature and of 138.9 $mAhg^{-1}$ at the higher temperature of 55 °C, while the initial discharge capacity of $LiMn_2O_{3.95}Br_{0.05}$ is 136.5 $mAhg^{-1}$ at ambient temperature and 119.2 $mAhg^{-1}$ at high temperature (55 °C); in addition, the rate performance of $LiMn_2O_{3.95}Br_{0.05}/SiO_2$ is excellent too.

Experimental procedure

Preparation Stoichiometric lithium acetate, manganese acetate, and lithium bromide were mixed with polyethylene glycol 400(worked as dispersants) in an agate mortar and ground with a pestle for 1 h, in order to make them react to reach the best possible homogeneity. Then the mixtures were dried at 120 °C for 8 h, and heat-treated at 450 °C for 1 h to obtain the precursors. The samples of $LiMn_2O_{3.95}Br_{0.05}$ were obtained by calcining the precursors at 800 °C for 10 h.

Amounts of ethyl orthosilicate were dissolved in 40 ml distilled water and 10 ml ethanol mixture, into which 1 g of the obtained precursors was dispersed. The mixture was churned up for 8 h at ambient temperature and dried at 80 °C to gain a kind of gray powder. The final samples of $LiMn_2O_{3.95}Br_{0.05}/SiO_2$ were obtained by calcining the gray powders at 800 °C for 10 h.

Characterization The crystalline phase of the resulting materials was analyzed by powder X-ray diffraction (XRD; MXP18AHF, MAC, Japan), which was carried out using Cu Kα radiation (λ=1.54056 Å). The grain size and morphology of the samples were observed using transmission electron microscopy (TEM; H-600, Hitachi, Japan). The working electrodes were fabricated by mixing the active materials with acetylene black and polyvinylidine fluoride at a weight ratio of 85:10:5 to form slurry, then the slurry was pasted on Al foil to form the electrode. The prepared electrode sheets were dried at 120 °C in a vacuum oven for 12 h. The electrochemical behavior of the test materials was examined via CR2032 coin-type cells with lithium metal counter electrode, microporous polyethylene (Celgard 2400) as the separator, and 1 M $LiPF_6$ in a mixture of ethylene carbonate and dimethylcarbonate (1:1 by volume) as the electrolyte. The whole assembly process was carried out in an argon-filled glove box. Cyclic voltammetry measurements (CVs) were measured at a scan rate of 0.1 mVs^{-1} from 3.0 to 4.35 V, using a CHI660B electrochemical workstation (CHI, 660B, Chenhua, China). The charge/dishcharge cycling was performed within a voltage range of 3.0–4.35 V on a battery test instrument (CT2001A, Land, China) at ambient temperature and a higher temperature (55 °C).

Results and discussion

The XRD patterns of $LiMn_2O_{3.95}Br_{0.05}$ and $LiMn_2O_{3.95}Br_{0.05}/SiO_2$ are shown in Fig. 1. From Fig. 1, we can see that the two samples have the features of the spinel structure with Fd3m space. All the peaks of the two samples are in good agreement with the standard of the JCPDS card (No. 35-0782), with no MnO_2 phase detected (shown in Fig. 1). The sharp peaks confirm the high crystallinity of the products. No SiO_2 peaks can be observed due to the little amounts.

The TEM of the two samples can be seen from Fig. 2. The sample of $LiMn_2O_{3.95}Br_{0.05}$ is composed of irregular nanoparticles, with diameter of about 100–200 nm. The edges of the particles are not smooth, however, after coating with SiO_2, the particles of the sample become more regular, and we can see the edges of the faceted crystallites become rounded, indicating the presence of

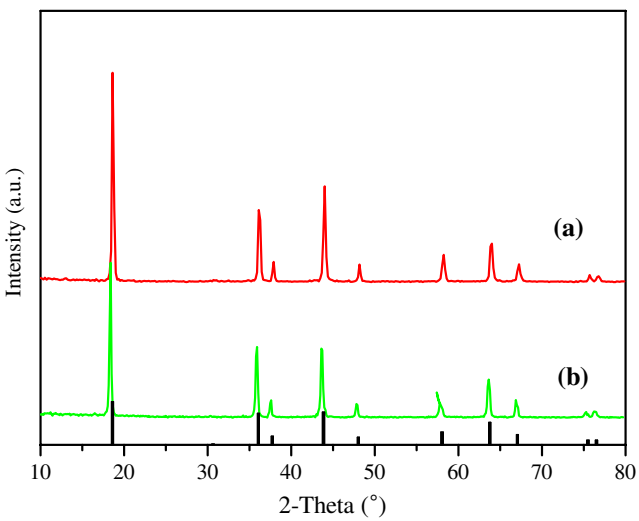

Fig. 1 The XRD patterns of **a** $LiMn_2O_{3.95}Br_{0.05}$ and **b** $LiMn_2O_{3.95}Br_{0.05}/SiO_2$

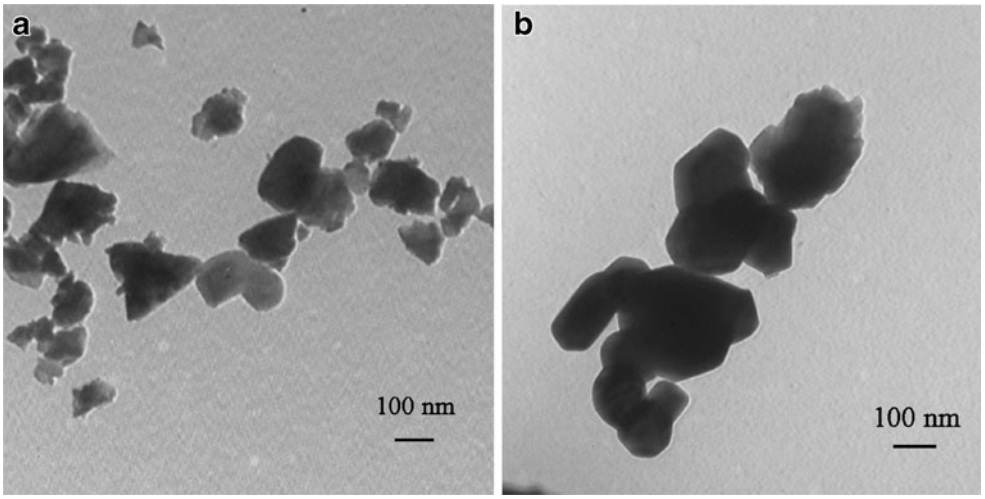

Fig. 2 TEM of **a** $LiMn_2O_{3.95}Br_{0.05}$ and **b** $LiMn_2O_{3.95}Br_{0.05}/SiO_2$

coating layer. According to the experimental method, the coating layer can be recognized as SiO_2 film.

The electrochemical properties of the $LiMn_2O_{3.95}Br_{0.05}$ and $LiMn_2O_{3.95}Br_{0.05}/SiO_2$ were investigated by cyclic voltammetry and galvanostatic cycling. CVs were recorded at ambient temperature in the 3.0–4.35 V range at a scan rate of 0.1 mVs^{-1}. The results are shown in Fig. 3. As can be seen in Fig. 3, all the samples own two pairs of peaks, which are observed in both anode and cathode scans, and the integrated areas during the anodic and cathodic process are almost equal, indicating good reversibility of the electrochemical reaction. Otherwise, we can see that the peak current of the sample $LiMn_2O_{3.95}Br_{0.05}/SiO_2$ is higher than the sample $LiMn_2O_{3.95}Br_{0.05}$, which indicate that the product with SiO_2 layer might have the better electrochemical activity.

Charge/discharge cycling measurements of the two samples were carried out in the voltage of 3.0–4.35 V (vs.Li) at a current density of 0.5 C at ambient temperature and a high temperature of 55 °C. The results are reported in terms of specific capacity versus cycle number (Fig. 4), voltage versus lithium concentration (x in $Li_xMn_2O_{3.95}Br_{0.05}/SiO_2$) at constant current (Fig. 5) and voltage versus the differential capacity (dQ/dV) during the initial charge and discharge processes (Fig. 5), as well as cycling performance.

Figure 4 displays the cycling performance of the two samples at ambient temperature. We can see that the initial discharge capacities of $LiMn_2O_{3.95}Br_{0.05}$ and $LiMn_2O_{3.95}Br_{0.05}/SiO_2$ are 136.5 $mAhg^{-1}$ and 145.3 $mAhg^{-1}$, respectively, which are less than the theoretical value (148 $mAhg^{-1}$), that's because at practical potentials (<5 V vs. Li/Li^+), it is impossible to extract all the lithium electrochemically [13]. And after 50 cycles, the discharge capacities of $LiMn_2O_{3.95}Br_{0.05}$ and $LiMn_2O_{3.95}Br_{0.05}/SiO_2$ remained 102.2 $mAhg^{-1}$ and 110.8 $mAhg^{-1}$, respectively,

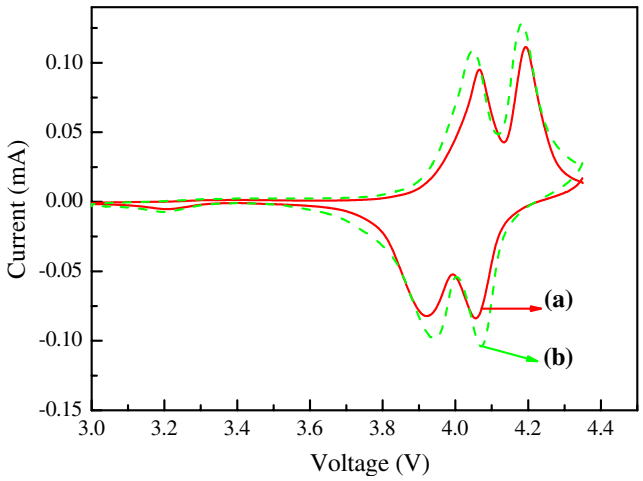

Fig. 3 Cyclic voltammetry of **a** $LiMn_2O_{3.95}Br_{0.05}$ and **b** $LiMn_2O_{3.95}Br_{0.05}/SiO_2$

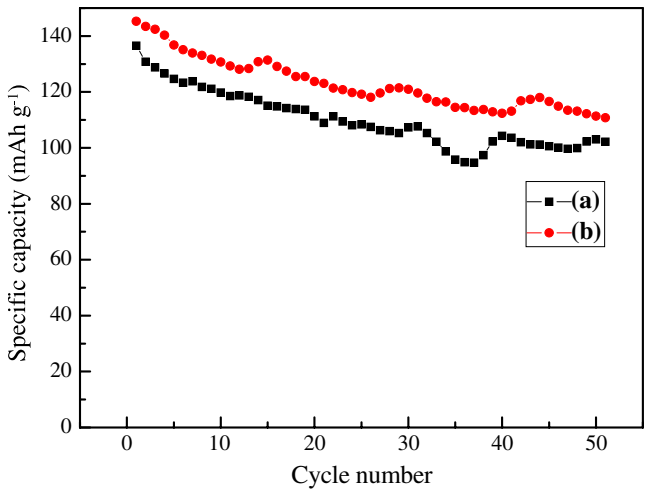

Fig. 4 The electrochemical cycling performance of **a** $LiMn_2O_{3.95}Br_{0.05}$ and **b** $LiMn_2O_{3.95}Br_{0.05}/SiO_2$ at ambient temperature

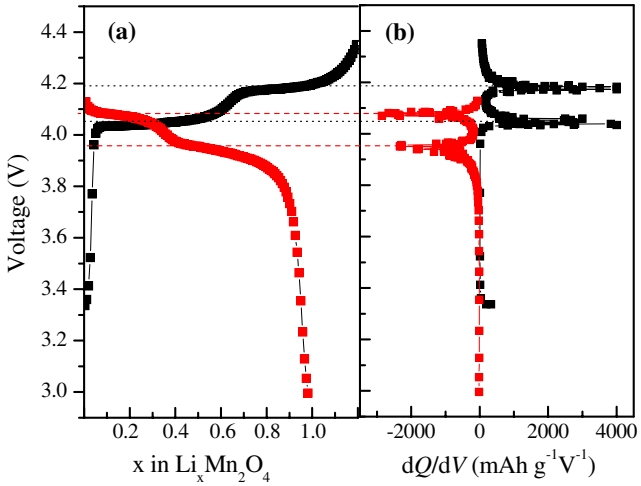

Fig. 5 **a** First cycle charge/discharge profiles of the $LiMn_2O_{3.95}Br_{0.05}/SiO_2$ at ambient temperature and **b** the differential capacity, dQ/dV (mAh$g^{-1}V^{-1}$), plots extracted from **a**

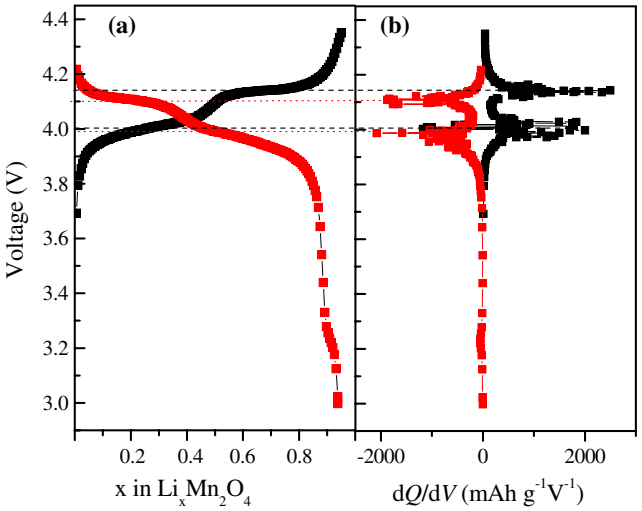

Fig. 7 **a** First cycle charge/discharge profiles of the $LiMn_2O_{3.95}Br_{0.05}/SiO_2$ at high temperature of 55 °C and **b** the differential capacity, dQ/dV(mAh$g^{-1}V^{-1}$), plots extracted from **a**

indicating that the $LiMn_2O_{3.95}Br_{0.05}/SiO_2$ samples have further improved the initial capacity and cycle performance, which is consistent with the CV measurements.

For the $LiMn_2O_{3.95}Br_{0.05}/SiO_2$ electrode in Fig. 5a, we can see that, during the first charge process, there are two obvious voltage plateaus observed at 4.05 V and 4.17 V; they correspond to the following different electrochemical reactions,

$$LiMn_2O_4 \rightleftarrows Li_{1/2}Mn_2O_4 + 1/2Li \quad (1)$$

$$Li_{1/2}Mn_2O_4 \rightleftarrows Mn_2O_4 + 1/2Li \quad (2)$$

A clear indication of the two reactions can be observed during the discharge process too. Meanwhile, it can be seen in Fig. 5, that the first discharge capacity of $LiMn_2O_{3.95}Br_{0.05}/SiO_2$ is 145.3 mAhg^{-1}, which is very close to the theoretical capacity of the $LiMn_2O_4$. This shows that about 0.98 mole Li^+ was extracted from the spinel matrix (as shown in Fig. 5a). The phenomenon that the capacity during the charge process appears larger than during discharge may attribute to a parasitic process, such as water oxidation [14, 15]. The voltages versus dQ/dV curves of the $LiMn_2O_{3.95}Br_{0.05}/SiO_2$ electrode clearly indicate the different nature of the two electrochemical processes, as shown in Fig. 5b. The sharp peaks observed in these curves correspond to the flat plateau seen in Fig. 5a. During the charge process, the first peak, at potential ranging from 4.03–4.12 V, displays a bell-shaped peak at 4.05 V, which

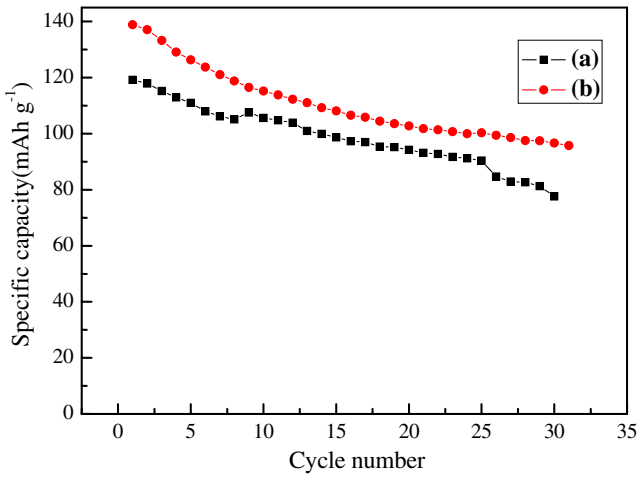

Fig. 6 The electrochemical cycling performance of **a** $LiMn_2O_{3.95}Br_{0.05}$ and **b** $LiMn_2O_{3.95}Br_{0.05}/SiO_2$ at high temperature of 55 °C

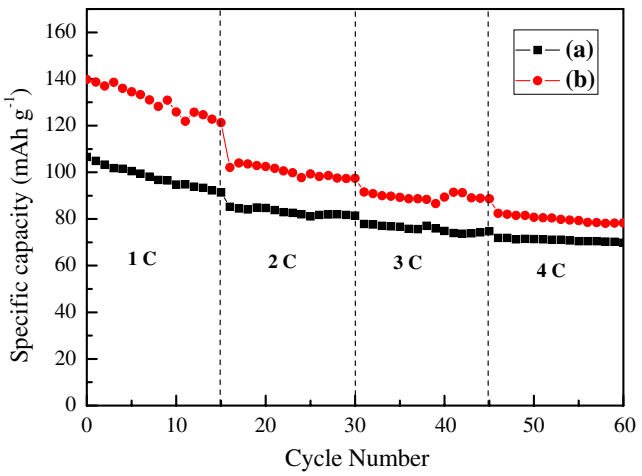

Fig. 8 Cycling and rate performance of **a** $LiMn_2O_{3.95}Br_{0.05}$ and **b** $LiMn_2O_{3.95}Br_{0.05}/SiO_2$ at ambient temperature

has full width at half-maximum (FWHM) of 30 mV, while the latter process shows a spike peak at 4.17V, with just 17 mV in FWHM. The difference between the two processes is also evident during the discharge scan, in which they occur at potential of 4.08 and 3.95 V, with FWHM of 112 and 120 mV, respectively. The potential drop between the charge and discharge process is only 95 mV at the rate of 0.5 C, indicating the fast kinetics of the system [15].

The poor cycling behavior of the pure $LiMn_2O_4$ is attributed to an asymmetric lattice expansion/contraction of the $LiMn_2O_4$ electrode during charge/discharge reactions. This lattice distortion is largely a result of the Jahn–Teller effect of the Mn^{3+}. This effect transforms of the cubic crystal symmetry of the spinel electrode into tetragonal symmetry [16–18]. In our work, the SiO_2 clung to the surface of the active particles, which have reduced the structure change of the products during the electrochemical processes effectively, so the electrochemical performance improved.

To investigate the elevated temperature stability of the two samples, their variation of discharge capacity with cycle number at 55 °C were tested, which can be seen in Fig. 6. The samples remain to be in high capacity and good retention; the initial discharge capacities of $LiMn_2O_{3.95}Br_{0.05}$ and $LiMn_2O_{3.95}Br_{0.05}/SiO_2$ are 119.2 mAh g^{-1}, 138.9 mAhg^{-1}, 77.6 mAhg^{-1} and 95.8 mAhg^{-1} after 30 cycles, and the capacity retentions are 65.1% and 69.0%, respectively, which confirm the better electrochemical behavior of $LiMn_2O_{3.95}Br_{0.05}/SiO_2$.

To further investigate the superiority of the $LiMn_2O_{3.95}Br_{0.05}/SiO_2$ electrode in the higher temperature, voltage versus lithium concentration(x in $Li_xMn_2O_{3.95}Br_{0.05}/SiO_2$) at constant current and voltage versus the differential capacity (dQ/dV) during the first charge and discharge process are obtained. As shown in Fig. 7a, both the curves are similar to the curves obtained at ambient temperature, indicating the same electrochemical processes. During charge process, there are two voltage plateaus in Fig. 7a, which correspond to the peaks of voltage versus the differential capacity (dQ/dV) in Fig. 7b, are observed at 4.01 V and 4.14 V. The same condition occurs at 3.99 V and 4.10 V during the discharge process. The potential drop between the charge and the discharge process is only 30 mV, which is lower than that in the ambient temperature, indicating that the kinetics of the system become much faster in higher temperature. The capacity loss at high temperature is due to the following factors: (1) an unstable two-phase structure coexists in the high voltage region for lithium-ion insertion/extraction, (2) manganese slowly dissolves in the electrolyte solution, and (3) the electrolyte solution decomposes on the electrode [19]. The improved electrochemical performance in the elevated temperature of the as-prepared samples can be ascribed to the special structure of the samples with the SiO_2 shell, which successfully hinders the contact of the electrolyte solution and the active material and lowers the rate of manganese to dissolve in the electrolyte availability.

The more remarkable advantage of the materials is the high rate capability, as shown in Fig. 8 ranging from 1 C to 4 C, the sample of $LiMn_2O_{3.95}Br_{0.05}/SiO_2$ also show the better electrochemical process than the other one, with stable reversible capacities around 139.8 mAhg^{-1}, 104.3 mAhg^{-1}, 90.9 mAhg^{-1}, and 82.7 mAhg^{-1}, at current densities of 1 C, 2 C, 3 C, and 4 C, respectively. While the capacities of the sample without SiO_2 coating are 101.1 mAhg^{-1}, 81.5 mAhg^{-1}, 72.9 mAhg^{-1}, and 67.2 mAhg^{-1}. The rate cycling performance further confirmed the superiority of the special structure of SiO_2 coating $LiMn_2O_{3.95}Br_{0.05}$.

Conclusion

$LiMn_2O_{3.95}Br_{0.05}$ and $LiMn_2O_{3.95}Br_{0.05}/SiO_2$ composites were prepared successfully by solid-state reaction methods. $LiMn_2O_{3.95}Br_{0.05}/SiO_2$ composites show high initial discharge capacities and rate performance. Measurement results show that the material can deliver high reversibility capacities of 145.3 mAhg^{-1} at ambient temperature, and 138.9 mAhg^{-1} at high temperature (55 °C), at a current density of 0.5 C, with good capacity retention.

Acknowledgment This work was supported by the Nature Science Foundation of Xinjiang Province (Grant Nos. 200821121 and 200821122), the National Natural Science Foundation of China (Grant Nos. 20866009 and 20861008), and Technological People Service Corporation (2009GJG40028).

Reference

1. Deng B, Nakamura H, Zhang Q, Yoahio M, Xia Y (2004) Electrochim Acta 49:1823
2. Zheng ZS, Tang ZL, Zhang ZT, Shen WC, Lin YH (2002) Solid State Ionics 148:317
3. Arrebala J, Caballero A, Hernan L, Morales J (2007) J Electrochem Soc 154:178
4. Hu G, Wang X, Chen F, Zhou J, Li R, Deng Z (2005) Electrochem Commun 7:383
5. Li X, Cheng F, Guo B and Chen J (109) J Phys Chem B 109:14017
6. Lin YM, Wu HC, Yen YC, Guo ZZ (2005) J Electrochem Soc 152:1526
7. Miao S, Kocher M, Rez P, Fultz B, Yasunori (2005) J Phys Chem B 109:23473
8. Choi HJ, Lee K-M, Lee JG (2001) J Power Sources 103:154
9. Sun YK (2000) Electrochem Commun 2:6
10. Thirunakaran R, Kim KT, Kang YM, Seo CY, Lee JY (2004) J Power Sources 137:100

11. Huang Y, Jiang R, Bao S, Cao Y, Jia D (2009) Nanoscale Res Lett 4:353
12. Song L, Li YL, Tang H, Zhang KL (2006) Norganic Chemicals Industry 38:20
13. Huang Y, Jiang R, Bao S, Dong Z, Cao Y, Jia D, Guo Z (2009) J Solid State Electrochem 13:799
14. Jiao F, Bao J, Hill AH, Bruce PG (2008) Angew Chem 120:9857
15. Kim DK, Muralidharan P, Lee HW, Ruffo R, Yang Y (2008) Nano Lett 8:3948
16. Thackeray MM, Picciotto LAD, Kock AD, Johnson PJ (1985) J Power Sources 21:1
17. Winter M, Besenhard JO, Spahr ME, Novak P (1998) Adv Mater 10:725
18. Yamada A, Tanaka M (1995) Mater Res Bull 30:715
19. Xia Y, Yoshio M (1997) J Power Sources 66:129